coatings

MDPI

Article

The Immobilization of Laccase on Mixed Polymeric Microspheres for Methyl Red Decomposition

Ludmila Aricov [1], Adina Raducan [2], Ioana Catalina Gifu [3], Elvira Alexandrescu [3], Aurica Precupas [1], Alexandru Vincentiu Florian Neculae [1], Raluca Marieta Visan [1], Alina Morosan [4] and Anca Ruxandra Leonties [1,*]

1 "Ilie Murgulescu" Institute of Physical Chemistry, Romanian Academy, 060021 Bucharest, Romania
2 Department of Physical Chemistry, Faculty of Chemistry, University of Bucharest, 030018 Bucharest, Romania
3 National Institute for Research and Development in Chemistry and Petrochemistry—ICECHIM, 060021 Bucharest, Romania
4 Department of Organic Chemistry "Costin Nenițescu", Faculty of Applied Chemistry and Materials Science, University Politehnica of Bucharest, 011061 Bucharest, Romania
* Correspondence: aleonties@icf.ro

Abstract: Means of eliminating water pollutants or transforming them into less hazardous compounds by green catalysis are desired. The current work was developed with the goal of discovering supports suited for laccase (Lc) immobilization. The effect of the chitosan (CS) molecular weight (Mw) or the polyacrylic acid (PAA) addition was evaluated in microsphere formulation and enzyme immobilization by ESEM, rheology, operational stability, and kinetics. As a practical application, the synthesized products were tested in the methyl red (MR) decomposition and the product identification was performed by high-resolution mass spectrometry. Depending on the required properties, the laccase activity profile (pH, temperature, storage, and Michaelis–Menten parameters) and rheological strength can be modulated by varying the molecular mass of CS or by adding PAA in the support formulation. The immobilized products having the best features regarding MR degradation and recycling abilities were the medium Mw CS microspheres and the system with low Mw CS complexed by PAA, respectively. The degradation mechanism of the dye was proposed accordingly with the identified products by mass spectroscopy. The findings emphasize the potential of the proposed immobilization products to be exploited as viable biocatalysts for dye-contaminated water.

Keywords: *Trametes versicolor* Laccase; immobilization; glutaraldehyde; low molecular weight chitosan; medium molecular weight chitosan; polyacrylic acid; methyl red decomposition

Citation: Aricov, L.; Raducan, A.; Gifu, I.C.; Alexandrescu, E.; Precupas, A.; Neculae, A.V.F.; Visan, R.M.; Morosan, A.; Leonties, A.R. The Immobilization of Laccase on Mixed Polymeric Microspheres for Methyl Red Decomposition. *Coatings* **2022**, *12*, 1965. https://doi.org/10.3390/coatings12121965

Academic Editor: Fengwei (David) Xie

Received: 11 November 2022
Accepted: 9 December 2022
Published: 15 December 2022

1. Introduction

Plenty of substances are required to meet the growing demands of the expanding markets such as health, pharmaceutical, and fine chemical companies [1,2]. Catalysts are used to respond quickly to the demand for such materials and to accelerate growth in the chemical industry [3,4]. Scientists are increasingly concerned about environmental issues, and they are investigating sustainable alternatives to conventional catalysts, including the use of enzymes [5]. Enzymes are proteins with interesting properties, capable of catalyzing various reactions in mild environmental conditions. From the multitude of enzymes with commercial potential, laccases are remarkable due to the wide range of applications in which they are used—such as biosensors, lignin degradation, wastewater treatment, etc. [6–10]. In any case, exploiting laccases to their true value is difficult, due to the low stability in the presence of harsh chemicals and physical stressors. Although effective in the reactions they catalyze, these enzymes have a high production cost [11] and are difficult to recover from liquid media where the majority of reactions take place [12]. To address these issues, enzymes can be immobilized on solid support materials. The literature presents various methods of laccase stabilization—such as cross-linking, absorption, and

entrapment [13]. Regarding the support, a wide range of materials from metals to polymers can be shaped into various structures with sizes of quantum dots up to centimeters. The most effective method to immobilize laccase is by chemical linking to support, using agents such as glutaraldehyde, EDC, DCC, cyanuric chloride, and epichlorohydrin [14]. For a successful immobilization, both the cross-linker and support must be carefully chosen to avoid unwanted phenomena such as low immobilization yields, deactivation of the enzyme catalytic site, destruction of the protein structure, or even of the binding support [13,15]. While taking into account the above-mentioned features, there is interest in obtaining and studying new types of supports which are resistant to environmental factors and which also allow a good recycling of the immobilized enzyme. If these conditions are met, operational costs can be reduced, and enzymes become a viable option for catalysts [16].

Chitosan is a natural polysaccharide, synthesized by deacetylation of chitin, extracted from marine or plant-based sources (crustaceans, insects, microorganisms, fungus, seaweed) [17–20]. This type of biopolymer is often used as a material support to immobilize enzymes. Using the coagulation method [21], spheres of different sizes can be obtained which can later be used as supports to immobilize the case. Aspects such as the CS concentration used, the degree of acetylation and the CS molecular mass, the strength of the base in the coagulation bath, and the amount of time the microsphere is left for coagulation must all be taken into consideration in order to have an adequate support for enzyme immobilization. Even so, after optimizing the parameters for obtaining the support, at low pH or in the presence of physical stressors (high temperature or friction) the chitosan microspheres become brittle. One way to stabilize the chitosan supports is to provide a hard core, as found in core–shell systems [22], or to generate reinforcement of the structure by mixing it with another type of polymer [23]. The latter method has advantages in terms of simplicity, and also if a low-cost secondary polymer is used in the synthesis may be cost efficient. When polyacrylic acid (PAA) and CS are mixed together, microspheres with good resistance to physical and chemical stressors can be formed [24]. A prior investigation of polymer microspheres made of CS and PAA shown that the addition of PAA significantly increases the resistance to deformation [24]. The molecular weight of polymers is another important parameter that can influence their solubility and reactivity, thus modulating their practical applicability. In a recent scientific paper related to antitumor activities of CS–selenium nanoparticles, it was demonstrated that CS with the highest molecular weight had the best stabilization effect upon the nanoparticles, while easily releasing the cytotoxic compound Se0 against HepG2 cells via electrostatic effect [25]. Another study showed that both concentration and molecular mass of CS can affect the stability and release profile of curcumin loaded liposomes [26].

The present study was designed with the aim of finding a new support, which is suitable for the immobilization of laccase from *Trametes versicolor* via cross-linking with glutaraldehyde (GA). Chitosan with low or medium molecular weight (LCS and MCS) and their mixture with polyacrylic acid (PAA) were used. All products were analyzed by ESEM and rheological methods. The operational stability and kinetic profiles of the immobilized laccase were investigated with a classic substrate 2,2′-Azino-bis(3-ethylbenzothiazoline-6-sulfonic acid) diammonium salt (ABTS). Methyl red (MR) is a chemical dye that affects humans and animals as shown by recent studies [27,28]. Initially, a molecular docking study was conducted to determine the type of interaction that occurs between laccase and this hazardous dye. Then, the ability of the immobilized products to degrade the toxic MR in a mediated reaction was evaluated in terms of degradability and recyclability properties. The identification of the reaction products resulting from MR degradation was made using high resolution mass spectrometry.

2. Materials and Methods

2.1. Materials

Wako Pure Chemical Industries Ltd., in Osaka, Japan, provided the Poly (acrylic acid) (PAA, 25%, wt. aqueous solution) with Mw 166 kDa [29]. Low molecular weight

and medium molecular weight chitosan (LCS and MCS, 75–85% deacetylated), acetic acid, hydrochloric acid (37%), sodium hydroxide, ethanol, glutaraldehyde, laccase from *Trametes versicolor* (0.78 U/mg, Mw 70 kDa [30]), citric acid, disodium phosphate, monosodium phosphate, 2-(4-Dimethylaminophenylazo) benzoic acid, 2,2′-Azinobis (3- ethylbenzothiazoline-6-sulfonic acid) diammonium salt (ABTS; 98%), and methyl red dye (MR) were all bought from Sigma-Aldrich.

2.2. Microsphere Preparation and Enzyme Immobilization

Chitosan with low or medium molecular weight was dissolved in 3% acetic acid in order to prepare stock solution of 3 wt %. The stock solution of PAA 3 wt % was prepared with water. All solutions were kept under magnetic string (250 rpm) for 24 h. Afterwards, the polymer solutions were mixed so that the final concentrations of 2 wt % LCS or MCS and 1 wt % PAA were obtained. A white gel was formed after combining the CS and PAA; hence, a few drops of 37% HCl solution were added to create homogeneous mixture. The mixtures were left overnight at room temperature under magnetic string (250 rpm). Using a microperfusion needle of type 25 G, the solution of LCS or MCS and their mixtures with PAA were extruded to create the beads in a coagulation bath filled with 250 mL of 1 M NaOH aqueous solution and 26% ethanol. The beads were left in NaOH for 2 h to solidify at 150 rpm. At the end of the solidification process the microspheres were washed with water until the pH was neutral. Four types of polymeric microspheres were obtained LCS, MCS, LCSPAA, and MCSPAA.

Each type of microsphere was treated with 0.75% Ga in phosphate buffer 0.2 M at pH = 6, for 3 h, under magnetic stirring (150 rpm) and at room temperature. The unreacted Ga was washed with water and sodium phosphate buffer. Finally, the beads were treated with laccase solution 1 mg/mL for 4 h under magnetic stirring (150 rpm) and at room temperature. A final wash with water to remove the free laccase was carried out and afterwards the microspheres were stored in phosphate buffer pH = 6 in the fridge. To calculate the amount of immobilized Lc onto 1 g of dry microspheres, a quantity of wet microsphere was dried.

2.3. Characterization

2.3.1. ESEM

The micrographs of the wet microspheres before and after treatment with glutaraldehyde and laccase were obtained by environmental scanning electron microscope (ESEM-FEI Quanta 200, Eindhoven, The Netherlands). The microspheres were positioned on metal stabs with double sided carbon conductive tape and analyzed at 2 Torr pressure and 20–30 kV applied voltage for the GSED detector.

2.3.2. Rheology

Oscillation rheological tests were completed on a Kinexus PRO rheometer equipped with a Julabo CF41 cryo-compact circulator, parallel-plate geometries of 20 mm and a solvent trap to prevent water evaporation. Firstly, the linear viscoelastic region (LVER) was evaluated at 25 °C using amplitude sweep stress measurement at 1 Hz. The LVER tests were followed by frequency sweep stress, where the frequency was between 0.1 and 40 Hz at 1 Pa.

2.4. UV–Vis Methodology

2.4.1. Laccase Assay

The spectrophotometric conditions—such as enzyme concentration and substrate, pH, and temperature—were chosen to be suitable for the kinetic investigation. The stock solutions had the following concentrations: 1 mg/mL free Lc solubilized in 0.1 M sodium phosphate buffer pH = 6; 6 mg/mL ABTS solubilized in citric buffer pH = 4; 0.1 mg/mL MR solubilized sodium phosphate buffer pH = 6 and 1.67×10^{-4} M NaOH. For experiments with immobilized enzymes, 0.05 g wet microspheres were used if not mentioned otherwise.

The reaction media was citrate buffer pH 4 (if not specified differently) and the final volume of 3 mL. The reaction was followed at 420 nm for the ABTS, while for the MR at 528 nm. For the MR decomposition, the ABTS (1.94×10^{-5} M) was used as an electron transfer mediator [31].

2.4.2. Active Laccase Content Estimation

The amount of active enzyme immobilized on the obtained microspheres was determined with a calibration curve. For this purpose, the Lc and ABTS stock solutions from Laccase assay section were used. The free Lc concentrations ranged between 10 and 100 µL while the ABTS was maintained constant at 20 µL. The extended kinetic curve of ABTS decomposition by Lc was obtained using the product concentration at 420 nm and the extinction coefficient of 36,000 M^{-1} cm^{-1}. A linear fitting procedure was applied to the initial portion of the extended curves for the determination of initial reaction rates (r_R^0). Finally, the obtained reaction rates were plotted as function of the considered Lc concentrations and the slope and intercept used to estimate the Lc immobilized on the LCS, MCS, LCSPAA, and MCSPAA polymeric microspheres.

2.4.3. Operational Stability

The measurements for pH, temperature, and storage time were conducted using the Laccase assay with modifications as follows: the temperature influence was studied between 25 and 70 °C at pH = 4, the pH was varied between 2.6–7 and temperature was kept constant at 25 °C, while the storage life was followed for 40 days using the laccase assay with pH = 4 and working temperature of 25 °C.

2.4.4. Michaelis–Menten kinetics

The effect of ABTS concentration on the immobilized enzymes was investigated. The ABTS concentration was of 2.50×10^{-5} up to 8.33×10^{-5} M, while for the immobilized enzyme 0.05 g of wet microsphere were used in each experiment. The Lineweaver–Burk plots were employed to calculate the Michaelis–Menten constant (K_m), the maximum rate (V_{max}) and the turnover frequency (k_{cat}) [32].

2.5. Molecular Docking

Fungal laccases contain four catalytic Cu atoms and the T1 Cu binding site, located near the protein surface, is known to be the substrate binding and oxidation site [33]. Molecular docking studies of the substrates (ABTS, methyl red) with the enzyme from *T. versicolor* were performed using AutoDock Vina software [34]. The crystal structure of laccase (PDB ID:1GYC) was obtained from the RCSB Protein Databank [35]. The structures of ABTS and methyl red were optimized using density functional theory with B3LYP functional and 6-31G* basis set by Gaussian03 software [36], as previously reported for other ligands [37,38]. AutoDock tools [39] were used to convert ABTS, methyl red and enzyme structures to pdbqt format [40]. The rotatable bond of ABTS and methyl red structures were automatically detected and assigned. Molecular docking of ABTS and methyl red, both in the absence and in presence of ABTS, in the active site of the enzyme was framed by a grid with the following coordinates: the center (X: 15.00, Y: 20, Z: 40), and the dimension (X: 40.00Å, Y: 40.00Å, Z: 40.00Å). The Lamarckian genetic algorithm (LGA) was applied for local optimization of molecular complexes. In order to study the different interactions between laccase and the selected substrates, the BIOVIA Discovery studio 2019 was used [41].

2.6. Practical Application

2.6.1. Discoloration of MR

The spectra between 200–800 nm were collected at fixed intervals in order to observe the MR degradation in time. For this experiment the immobilized enzyme concentration maintained constant at 1.5×10^{-5} M for all supports types which was determined from the

calibration curve. The reaction volume (3000 µL) contained 5 µL of ABTS and 100 µL MR. The reaction was followed until no modifications in spectra were observed. The absorbance of MR at 528 nm was considered 100%.

2.6.2. Degradation Product Identification

The XR FTMS Hybrid System QqFTMS mass spectrometry having a superconducting magnetsolariX XR 15T was used for the identification of MR degradation products with Lc. Using a Fourier transform–ion cyclotron resonance spectrometer—SolariX XR 15T (Bruker Daltonics, Bremen, Germany)—the high-resolution mass spectrometry analysis was performed. The samples were investigated by direct infusion and positive ESI ionization with a flow rate of 120 µL/h, nebulization gas being N2 at a temperature of 180 °C. The following parameters were used: pressure of 1.5 Barr N_2, flow rate of 5 L/min, 92–1500 m/z mass range and source voltage of 5500 V and the MS spectra collected using monoisotopic peak isolation.

2.6.3. Recyclability of Immobilized Laccase

The recyclability of immobilized products was completed in 5 cycles using MR. The assay mentioned at section Laccase assay was used with a slight modification: 100 µL MR and a concentration of enzyme was of 1.5×10^{-5} M were used for the free and immobilized Lc. After each cycle, the microspheres with immobilized Lc were washed with phosphate buffer. The first cycle's reaction rate was assumed to be 100%.

3. Results and Discussion

3.1. Microsphere Characterization

3.1.1. ESEM Measurements

ESEM measurements were performed to investigate how the molecular weight of CS and the addition of PAA alters the morphology of the microsphere surface. As a result, images of microsphere before and after Lc immobilization are shown in Figure 1.

We observed that the LCS microspheres are smooth and free of pores. There were no significant changes in the surface aspect after Ga treatment, whereas enzymatic treatment causes the appearance of some deposits on the surface. MCS microspheres have very small pores (1–5 micrometers) that disappear after being treated with Ga. The presence of whitish deposits was also found after binding the Lc. In a study concerning the synthesis of chitosan-lysozyme microspheres the authors showed that the white deposits are correlated with immobilized protein presence on the support surface [42]. According to previous research [24], the inclusion of PAA in the formulation of microspheres with LCS results in a porous surface with pores of varying sizes (5–30 micrometers). The Ga treatment smoothed the surface, whereas the Lc treatment produces reticulation. The smooth appearance of the microspheres containing MCS and PAA is maintained even after treatment with Ga. The surface then wrinkles as a result of the enzyme's binding to the support. Similar findings were reported for fungal laccase immobilization on glutaraldehyde cross-linked chitosan beads and was argued that the microsphere aspect is owed to the enzyme coupling to chitosan during the immobilization process [43].

3.1.2. Rheology

Water-based polymeric materials have also been studied from the point of view of viscoelastic behaviors. Figure 2 shows the response of the storage and loss moduli when the shear stress is applied at a constant frequency of 1 Hz, before and after the enzyme immobilization procedure on the polymeric support.

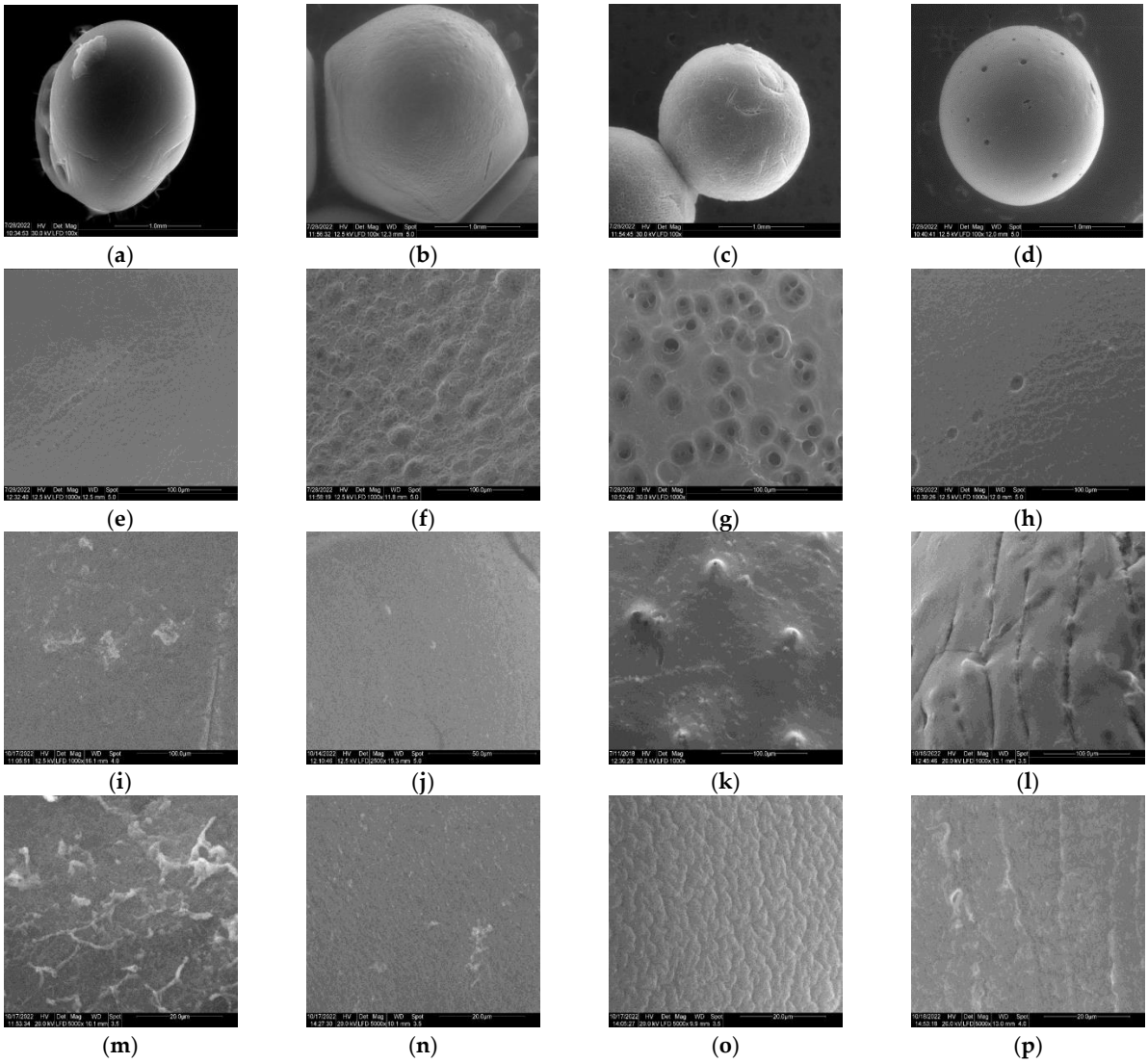

Figure 1. ESEM images of microspheres—(**a**) LCS, (**b**) MCS, (**c**) LCSPAA, (**d**) MCSPAA; their surfaces before immobilization—(**e**) LCS, (**f**) MCS, (**g**) LCSPAA, (**h**) MCSPAA; after Ga treatment—(**i**) LCSGa, (**j**) MCSGa, (**k**) LCSPAAGa, (**l**) MCSPAAGa; and after Lc immobilization—(**m**) LCSLc, (**n**) MCSLc, (**o**) LCSPAALc, (**p**) MCSPAALc.

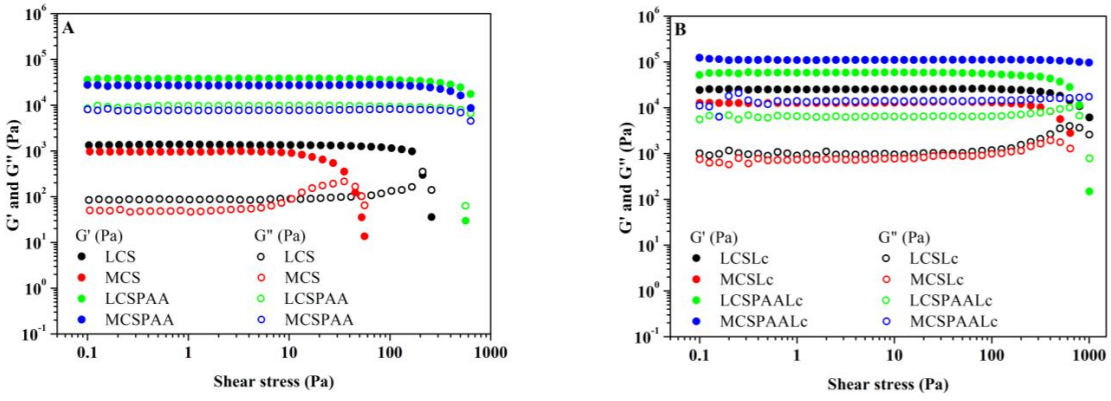

Figure 2. Effect of shear stress on storage (G′) and loss (G″) moduli for the studied microspheres: (**A**) before immobilization procedure and (**B**) after immobilization procedure.

The linear viscoelastic region before the laccase immobilization process (Figure 2A) highlights the effect of both the molecular mass of CS and the presence of PAA in the composition of the microspheres. The LCS and MCS systems present a less extensive LVER compared to those with PAA, especially the MCS which has a short linear region and is followed by a plastic deformation after 10 Pa. Meanwhile, the LCSPAA and MCSPAA systems have a very similar deformation behavior which is much better than those with only CS, marking the fact that PAA helps to increase the resistance to deformation—an effect given by the strong interactions between CS and PAA. After the immobilization stage (Figure 2B), all the microspheres undergo a positive transformation from a rheological point of view, increasing both the LVER and the value of the two viscoelastic moduli. The most obvious viscoelastic improvement, after immobilization with Lc, was found in the case of samples that contain only CS. Although the immobilization step leads to a significant increase in the resistance to deformation for LCS and MCS, they still do not exceed the mechanical resistance of microspheres with PAA. Therefore, we can assume that the presence of PAA most significantly influences the mechanical performance; however, the effect of the immobilization procedure cannot be neglected either, especially in the case of microspheres with only CS.

The effect of frequency on the two viscoelastic moduli was also investigated for polymeric supports. The data obtained in the case of the studied samples, before and after the immobilization stage, are shown in Figure 3.

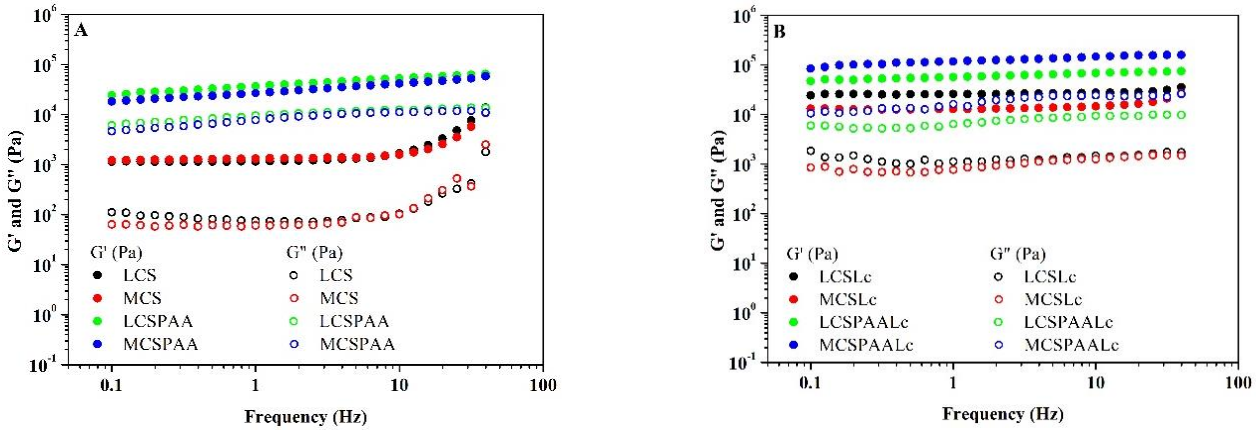

Figure 3. Effect of applied frequency on storage (G′) and loss (G″) moduli for the studied microspheres: (**A**) before immobilization procedure and (**B**) after immobilization procedure.

The rheological fingerprint highlights a viscoelastic gel character where the elastic component predominates (G′ > G″) over the entire frequency range, this behavior is found in the case of all the materials regardless of whether it is before or after Lc immobilization. The influence of the molecular mass of CS on the values of the storage and loss moduli is not significant, as can be seen in Figure 3, while the addition of PAA leads to the increase in the values of the rheological moduli. As was also observed in the case of the LVER region determination data, the Lc binding procedure on the polymeric supports lead to an improvement in the viscoelastic behavior of the studied gels, especially for the LCS and MCS systems. This can be attributed to the reaction environment during immobilization (ionic strength and pH), thus the buffer based on salts leads to the removal of water from the polymer networks, and the microspheres tend to shrink. The rheological study highlights the positive effect of the addition of PAA, but also of the immobilization stage. Thus, the MCSPAALc system, closely followed by LCSPAALc, presents the best rheological results.

3.2. Estimation of Active Immobilized Laccase Content on Immobilized Products

The amount of Lc immobilized on the polymeric supports was estimated using a calibration curve. Figure S1 from Supplementary Materials shows the calibration curve

representing the initial degradation rate of ABTS (r_R^0) as a function of the free Lc concentration. We found that the active amount of Lc immobilized on 1 g of polymeric support was 3.05 mg for MCS, followed by LCS with 2.24 mg, MCSPAA has 1.57 mg/g dry support, and 1.49 mg for LCSPAA. As can be seen, the presence of PAA reduces the amount of immobilized enzyme regardless of chitosan molecular weight. This is due to interactions between the two polymers, which results in a reduction in the number of amino groups available for binding laccase with GA. In addition, the amount of immobilized Lc was affected by the molecular mass of CS, a higher molecular mass allowing a better immobilization. A study regarding the immobilization of the same type of laccase onto amberlite beads revealed that a similar amount of immobilized enzyme found for the LCS support was found [44]. Similar amounts of laccase were obtained also for magnetic chitosan–clay composite beads [45]. In other studies, higher amounts of enzyme were deposited onto the supports, but different immobilization agent was used [24,32].

3.3. Operational Stability

The operational stability of the Lc immobilized on polymeric supports was evaluated by pH, temperature, and storage days. The obtained results are presented in Figure 4.

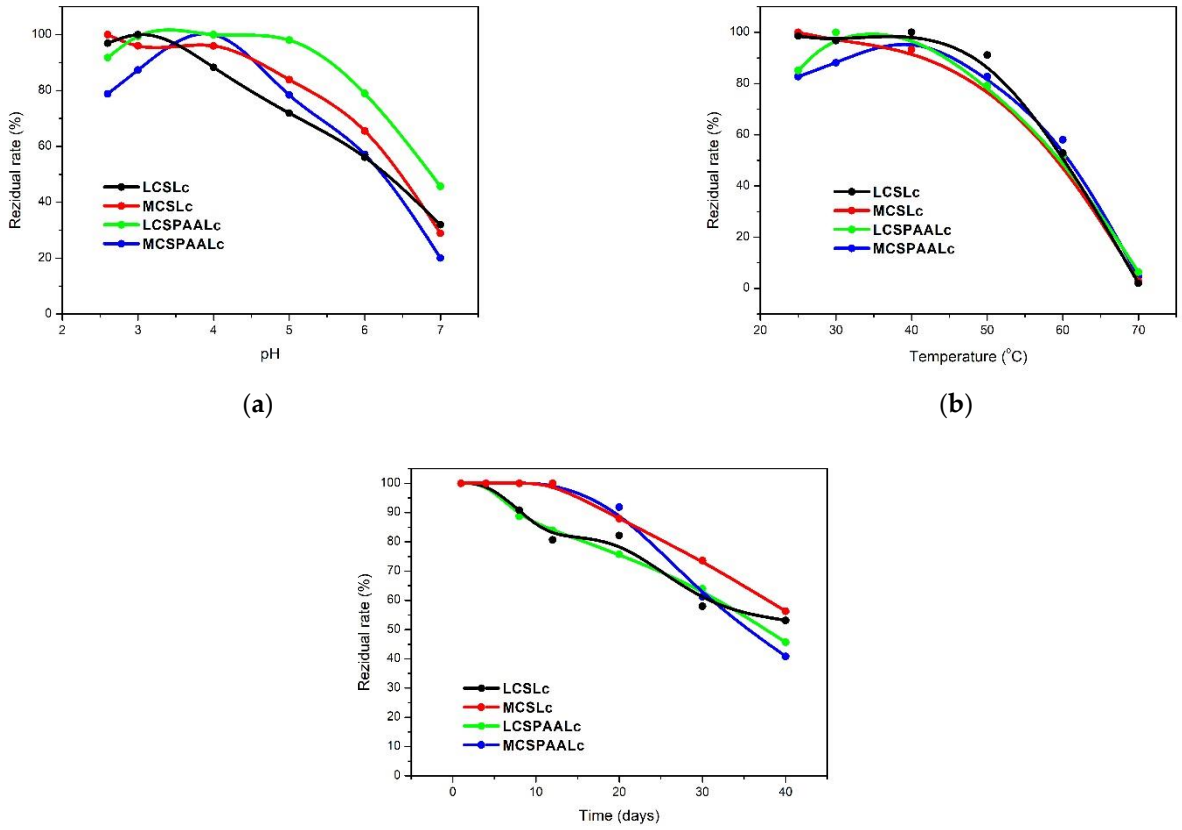

Figure 4. Effect of (**a**) pH, (**b**) temperature, and (**c**) storage on the immobilized Lc activity.

The pH profile (Figure 4a) of the immobilized LCS products reaches a maximum at pH = 3, after which the activity gradually decreases, with only 20% of the initial activity remaining at pH = 7. The MCS profile has a plateau between pH 2.6 and 4 where the bound Lc activity is almost constant (approximately 100%), then it decreases similarly to the LCS system. The pH profile of the LCSPAA system does not change significantly between 2.6 and 5, but between pH 6 and 7, a significant decrease from 80% to 40% is observed. MCSPAA exhibits an obvious maximum at pH = 4, then gradually decreases to approximately 20% at pH = 7. Regarding thermal behavior (Figure 4b), we noticed

that LCSLc and MCSLc activity has a plateau between 25 °C and 40 °C; and after 60 °C, the activity drops abruptly. The systems formed by LCSPAALc and MCSPAALc exhibit maximum activity at 30 and 40 °C, respectively, after these temperatures the behavior of the systems without PAA was respected. For 40 days, the storage behavior of immobilized Lc was studied (Figure 4c). It was observed that molecular weight of CS helps to keep the activity of the immobilized Lc on MCS or MCSPAA at about 90% for 20 days. Meanwhile, Lc immobilized on LCS and LCSPAA shows a similar behavior, but slightly lower activity compared to the microspheres containing CS of medium molecular weight. After 20 days, the activity of all immobilized products tends to decrease, although it still retains at least 40% of its initial activity at the end of the storage period.

3.4. Michaelis–Menten Kinetics

Using the Michaelis–Menten method, the impact of substrate concentration on the immobilized products was examined. The K_m forecasts the enzyme affinity toward the substrate while the V_{max} displays the enzyme maximal rate at which the active sites are saturated with substrate molecules. Another important parameter is the k_{cat} which is turnover number and is calculated the ratio between the V_{max} and the concentration of the active enzyme. Figure 5 shows the Lineweaver–Burk linear regressions obtained by representing the r_0^R for the immobilized products as function of the ABTS concentration.

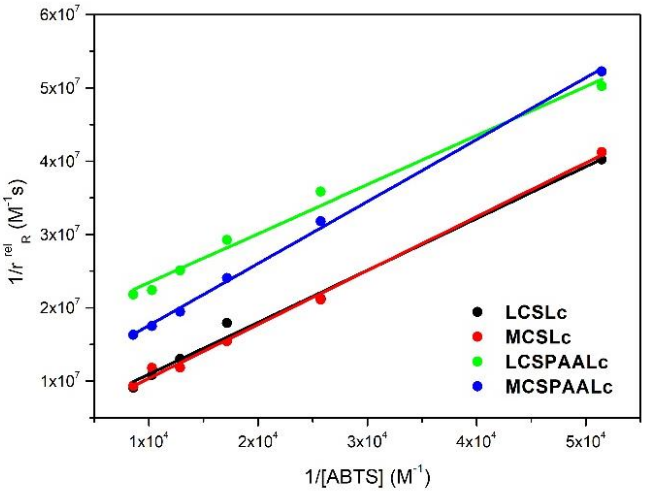

Figure 5. The Lineweaver–Burk plots of Lc immobilized on different microspheres (the lines are best fit of the obtained experimental data with the Michaelis–Menten model).

The obtained parameters—K_m, V_{max}, and k_{cat}—are listed in the Table 1.

Table 1. Michaelis–Menten parameters.

System	K_m (M)	V_{max} ($M \cdot s^{-1}$)	k_{cat} (s^{-1})	k_{cat}/K_m ($M^{-1}s^{-1}$)
LCSLc	1.85×10^{-4}	2.60×10^{-7}	4.23	2.29×10^{4}
MCSLc	2.45×10^{-4}	3.33×10^{-7}	3.91	1.60×10^{4}
LCSPAALc	0.40×10^{-4}	0.60×10^{-7}	2.49	6.22×10^{4}
MCSPAALc	0.93×10^{-4}	1.10×10^{-7}	2.61	2.82×10^{4}

We noticed that the K_m values for the studied systems are of the same order of magnitude, but higher than those of the free Lc, suggesting that the enzyme active site affinity toward the ABTS is slightly diminished [24]. This phenomenon is commonly reported in literature and is linked to the substrate molecules limited access to the enzyme active site as a result of potential alterations in the secondary and tertiary structure brought on by the immobilization process [46]. The V_{max} of all products has the same order of magnitude and compared to the free enzyme, the values are lower for the products with PAA, while

the LCS or MCS microspheres help the immobilized enzyme in gaining a better activity. The k_{cat} represents the turnover number which describes how many substrate molecules are transformed into products per unit of time by an enzyme molecule. The best turnover number was assigned to the enzyme immobilized onto LCS microspheres while the one onto MCS microspheres had similar value. The Lc immobilized onto mixed polymeric microsphere has the k_{cat} slightly lower implying that the immobilized Lc structure encounters diffusion limitation. This observation is in agreement with literature data reported [47,48]. Another approach to determine whether the immobilization procedure has an effect on enzyme activity is to estimate the specificity constant (k_{sp}). The k_{sp} is obtained by dividing the k_{cat} with K_m and is closely related to the catalytic efficiency of a given enzyme on a particular substrate. As a result, greater ratios are associated with higher catalysis rates. LCSPAALc had the highest k_{sp}, followed by the Lc immobilized on MCSPAA supports. The Lc immobilized on simple CS microspheres exhibited a reasonable k_{sp}, which agreed with free Lc [24]. Based on the values from Table 1, we can conclude that the microspheres containing MCS have a positive influence on the enzyme immobilization, providing a good turnover number, whereas the PAA addition in the microsphere formulation generates immobilized Lc with higher catalytic efficiency toward the studied substrate.

3.5. Molecular Simulation

Molecular docking was used to predict the optimum binding mode between ligand and receptor. The binding mode of ABTS and the active site of laccase was shown in Figure 6.

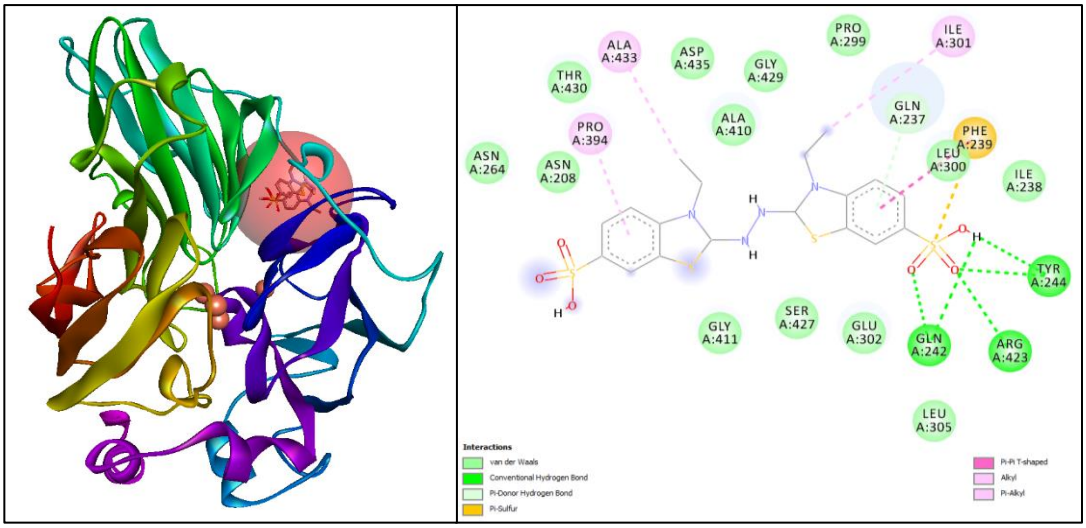

(**a**) (**b**)

Figure 6. Molecular docking of ABTS and laccase; (**a**) the substrate is presented as stick and balls and the enzyme as solid ribbon and (**b**) two-dimensional diagram, the close aminoacid residues are presented in green, dashed lines represent intermolecular interactions of different origin (hydrogen bonds—green lines; π-π/π-cation stacking—pink/purple lines; van der Waals interactions and other hydrophobic forces—light green lines).

The molecular docking results showed hydrogen bonds, electrostatic and hydrophobic interactions between ABTS and laccase. Four residues Gln242, Tyr244, Arg423, and Gln237 participated in the formation of hydrogen bonds with ABTS; whereas Phe239, Ala433, Ile301, and Pro394 present hydrophobic interactions with the substrate. The binding affinity of ABTS with the enzyme is -8.30 kcal mol^{-1}.

The binding mode of methyl red with laccase in the absence of ABTS was presented in Figure 7.

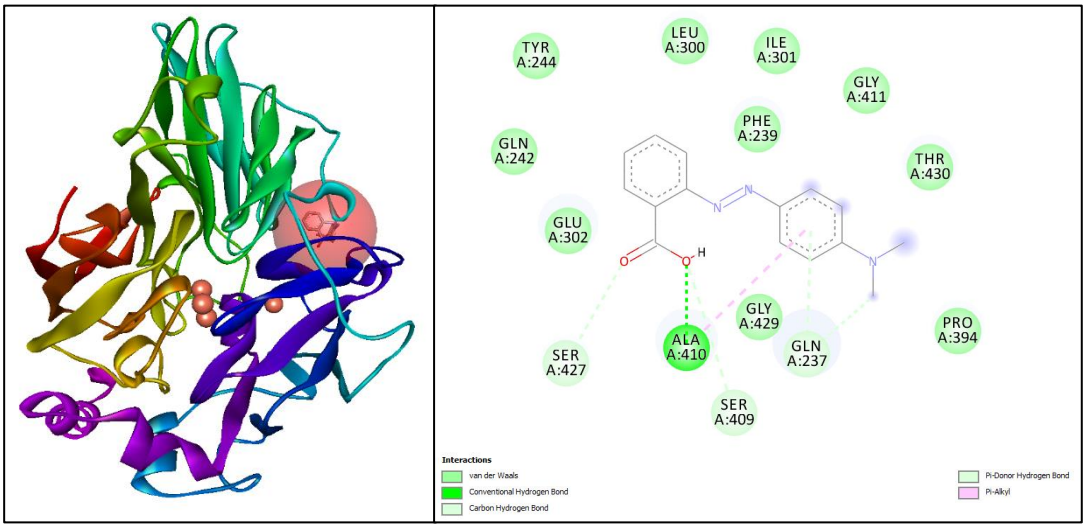

(**a**) (**b**)

Figure 7. Molecular docking of methyl red and laccase; (**a**) the substrate is presented as stick and balls and the enzyme as solid ribbon and (**b**) two-dimensional diagram, the close aminoacid residues are presented in green, dashed lines represent intermolecular interactions of different origin (hydrogen bonds—green lines; π-alkyl—pink line; van der Waals interactions and other hydrophobic forces—light green lines).

Methyl red binds at the active site of laccase with a lower binding affinity (−6.9 kcal mol^{-1}) than ABTS. Five hydrogen bonds and one hydrophobic interaction were noted between amino acid residues of laccase (Ala410, Ser409, Ser427, Gln237) and methyl red. When ABTS is already bound at the laccase binding site, the molecular docking results (Figure 8) revealed a decrease in methyl red binding affinity with the enzyme (−6.6 kcal mol^{-1}).

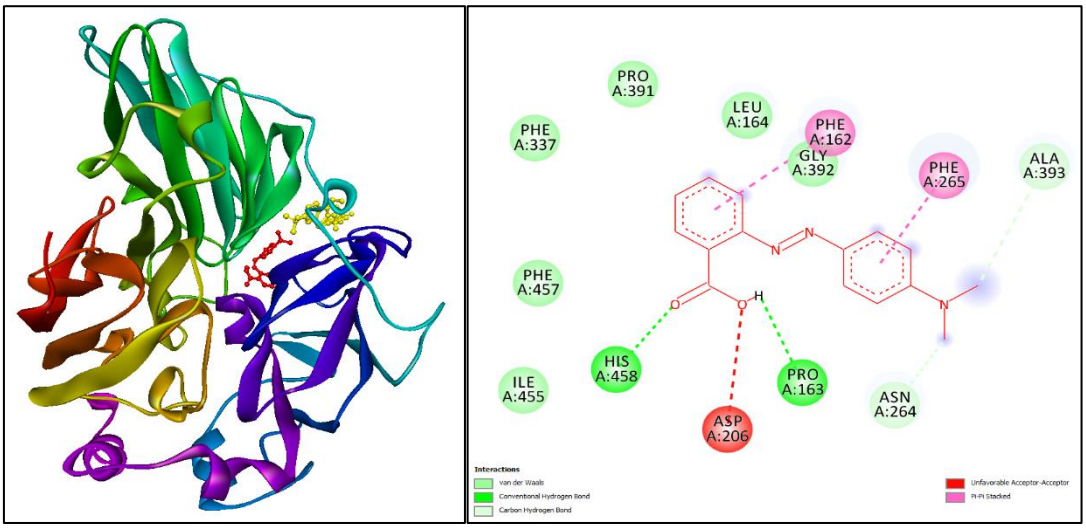

(**a**) (**b**)

Figure 8. Molecular docking of methyl red with ABTS and laccase; (**a**) methyl red is presented as stick and balls colored in yellow, ABTS as stick and balls colored in red and the enzyme as solid ribbon and (**b**) two-dimensional diagram, the close amino acid residues are presented in green, dashed lines represent intermolecular interactions of different origin (hydrogen bonds—green lines; van der Waals interactions—light green lines; hydrophobic forces—pink lines).

Hydrogen bonds between His458, Pro163, Ala393, and Asn264 and methyl red, and hydrophobic interactions with Phe162 and Phe265 were observed. It has been reported that N^{ε} H-atom of His458 was involved in the actual electron transfer [49] and Asp206 residue forms crucial interactions with laccase substrates.

3.6. Practical Application

Since the theoretical findings from molecular simulation were promising we studied the ability of the free and immobilized Lc to degrade the MR dye. This dye was chosen because research indicates that it is harmful (mutagenic or carcinogenic), pollutes water, and has an impact on both aquatic and human life [27]. As a result, eliminating MR or transforming it into less hazardous compounds by green catalysis is preferable.

3.6.1. Discoloration of MR and Recyclability

Expanding the laccase activity over a wide range of substrates may be carried out using redox mediators. In this particular case, MR catalysis with free or immobilized laccase was mediated by ABTS because MR degradation was a slow process. This type of reaction occurs when substrates are too large and may be sterically hindered, have poor affinity constants, or excessively high redox potentials in comparison to the free enzyme. Figure 9 depicts the breakdown of MR in the presence of ABTS and an immobilized or free enzyme followed spectrophotometrically at the wavelength λ = 525 nm. The concentration of MR chosen in this study is similar to that found in real water and is considered toxic for aquatic fauna and flora [50].

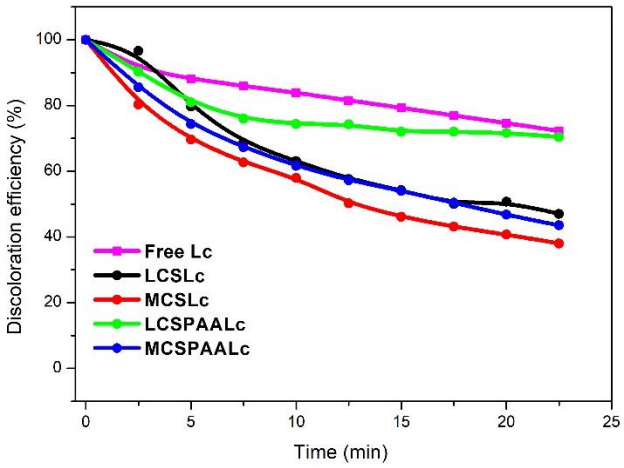

Figure 9. Degradation reaction of MR in the presence of free or immobilized Lc M and ABTS.

The results showed that—even if mediated—the reaction takes place slowly. Thus, free Lc and LCSPAALc degrade only 20% of the amount of MR in 20 min, while the rest of the products have a better degradation efficiency, reaching 70% for MCSLc. There are studies showing the degradation of MR by laccase is a slow process. Therefore, literature presents that actinobacterium from *Zhihengliuella* sp. ISTPL4 is able to degrade 98.87% of 0.5 mg/mL methyl red dye degradation in 12 h [28]. In another study, cross-linked laccase aggregates are able to degrade a similar amount of MR in 10 h [51].

Thus, we can say that the MCSLc product has the best features in the mediated degradation of MR both in terms of concentration and degradation time, suggesting that chitosan with medium molecular weight is beneficial for immobilization. Yet, the activity of the Lc immobilized onto LCS and MCSPAA cannot be neglected.

3.6.2. Recyclability of Immobilized Laccase

To be efficient, an immobilized product must resist numerous recycling cycles. Thus, Figure 10 shows the reusability of immobilized products in five cycles toward MR in the presence of ABTS.

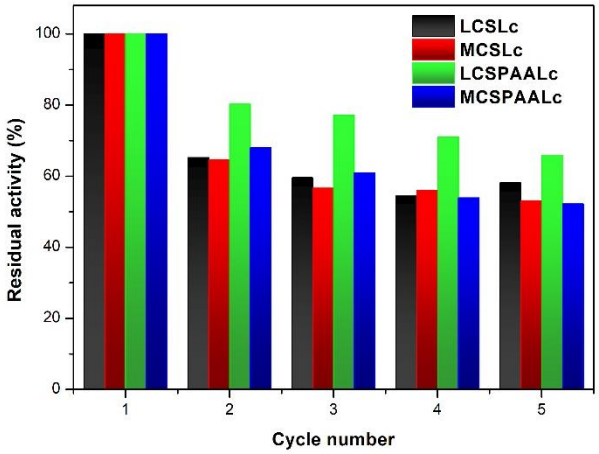

Figure 10. Reusability of immobilized products used for MR discoloration.

For all products, a decrease in activity was observed after the first cycle as follows: LCSPAALc decreased with 20%, MCSPAALc with 30% while LCSLc and MCSLc decreased with 35%. As the enzyme becomes less stable after the second batch cycle, it is possible that newly generated products or undegraded MR are responsible for the inactivation. Similar behavior has been observed for *Aspergillus* sp. laccase cross-linked on chitosan during syringaldazine degradation [52]. Interestingly, after the second cycle the activity is maintained almost constant, a decrease of less than 10% is observed after the fifth cycle. The enzyme activity loss during the recycling procedures was reported for other types immobilized laccase [32], and may be due to the accumulation of dye and/or reaction products into the active sites of the enzyme after repeated uses [24], or loss of enzyme molecules during each batch [53].

3.6.3. Degradation Product Identification

The reaction products of MR decomposition in presence of laccase were firstly investigated by UV–Vis spectrophotometry and the comparison between spectra is presented in Figure S2 from Supplementary Materials. Since the MR discoloration was mediated by ABTS, it was noticed that substrate competition appeared when the dye concentration dropped lower than the mediator one. The presence of the absorption maxima at 420 nm specific for the $ABTS^{\bullet+}$ radical was detected in all systems. We observed that at the end of the reaction time all spectra have similar peaks, and we concluded that the reaction mechanism is the same, regardless of microsphere composition or whether the enzyme was in the free or immobilized form.

The reaction products were identified by high-resolution mass spectrometry analysis and the obtained monoisotopic MS spectra are found in Figures S3–S6 from supplementary material. Initially, when the reaction started, the monoisotopic MS peaks of MR (1) and ABTS adduct with sodium ions were identified at 270.12 m/z (Figure S3) and 558.98 m/z (Figure S4.). As the reaction toked place, an intermediary partially reduced product (2) was identified having 272.13 m/z (Figure S5.). At the end of the reaction, the product with 311.12 m/z was identified as the adduct of N,N-Dimethyl-p-phenylenediamine (4) with citric acid (Figure S6) and the reaction mechanism is suggested in Scheme 1.

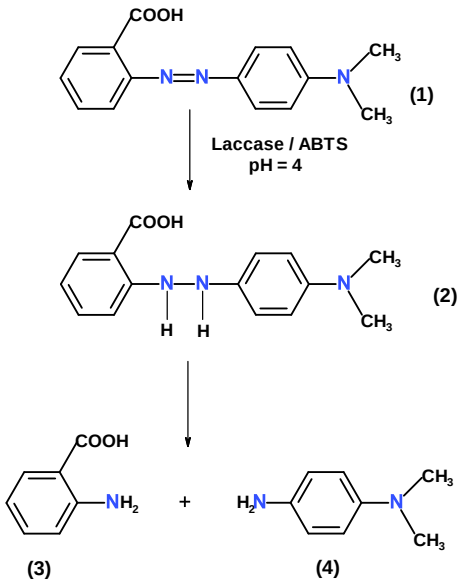

Scheme 1. Proposed degradation mechanism of MR in presence of Lc mediated by ABTS.

From the MS spectra, we proposed the mechanism described in Scheme 1. It was assumed that the degradation mechanism of MR by laccase in presence of ABTS, firstly implies the cleavage of the diazo bond and formation of a hydrazo derivative. Next, the reduction of the hydrazo bond takes place and is followed by the formation of aminobenzoic acid and dimethyl phenylenediamine.

Although N,N-Dimethyl-p-phenylenediamine is toxic in certain dosages, this substance is not considered to be either persistent [54], or bioaccumulated [55]. Therefore, in real life applications, this product may be further degraded using complimentary techniques such bacterial digestions [56,57], or even electrochemically [58]. The reaction product (3) was expected to be anthranilic acid which is not considered toxic for mammals [59], and was not found among the monoisotopic MS peaks of the decomposed MR solution.

4. Conclusions

The immobilization of laccase from *Trametes versicolor* was performed by glutaraldehyde crosslinking on microspherical supports. The water-based microspheres were formulated with pure chitosan having different molecular weights or by mixing them with polyacrylic acid. As shown by rheological measurements, the support resistance to mechanical stress was improved when the chitosan was complexed with polyacrylic acid. Surface modifications of the microspheres were observed by ESEM and generated by the type of chitosan, polyacrylic acid presence, and laccase immobilization. The catalytic performance of all immobilized products was also tuned by the support chemical content. Methyl red degradation was followed spectroscopically; and at the end of the reaction, the degradation products were identified. The high-resolution mass spectrometry revealed that the degradation products are less toxic than the parent compound. The findings highlight the unique properties of the presented materials, which might be employed in the immobilization of other enzymes or in the elimination of other harmful chemicals.

Supplementary Materials: The following supporting information can be downloaded at: https://www.mdpi.com/article/10.3390/coatings12121965/s1, Figure S1: The calibration curve of free laccase in presence of ABTS substrate. The straight line represented the best linear fit of the data; Figure S2. The UV-Vis spectra of MR in presence of ABTS and free and immobilized Lc after 20 min; Figure S3. The FT-ICR-MS spectra of MR (A. Buffer, B. MR, and C. Simulated spectra of MR); Figure S4. The FT-ICR-MS spectra of ABTS (A. Buffer, B. ABTS adduct with sodium ions, and C. Simulated spectra of ABTS); Figure S5. The FT-ICR-MS spectra of partially reduced MR (A. Buffer, B. Partially

reduced MR, and C. Simulated spectra of partially reduced MR); Figure S6. The FT-ICR-MS spectra of the N,N-Dimethyl-p-phenylenediamine (A. Buffer, B. N,N-Dimethyl-p-phenylenediamine with citric acid, and C. Simulated spectra of N,N-Dimethyl-p-phenylenediamine with citric acid).

Author Contributions: Conceptualization, methodology, validation, formal analysis, rheology investigation, data curation, writing–original draft preparation—L.A.; Formal analysis, kinetic analysis—A.R.; Formal analysis, SEM investigation, data curation—I.C.G.; Formal analysis, SEM investigation, data curation—E.A.; Methodology, software, molecular dynamics analysis, writing—original draft preparation—A.P.; Validation, formal analysis, UV–Vis investigation—A.V.F.N.; Validation, Formal analysis, UV–Vis investigation—R.M.V.; Validation, formal analysis, mass spectrometry investigation—A.M.; Conceptualization; methodology, formal analysis, UV–Vis investigation, resources; data curation, writing—review and editing, visualization, supervision, project administration, funding acquisition—A.R.L. All authors have read and agreed to the published version of the manuscript.

Funding: This work was supported by a grant of the Ministry of Research, Innovation and Digitization, CNCS—UEFISCDI, project number TE 68/2022, PN-III-P1-1.1-TE-2021-0418, within PNCDI III.

Institutional Review Board Statement: Not applicable.

Informed Consent Statement: Not applicable.

Data Availability Statement: Not applicable.

Acknowledgments: This work was supported by the Romanian Academy within the research program 'Colloids and dispersed systems' from 'Ilie Murgulescu' Institute of Physical Chemistry. We would also like to acknowledge the grant of the European Regional Development Fund through Competitiveness Operational Program 2014—2020, Priority axis 1, Project No. P-36-611, MySMIS code 107066—INOVABIOMED which made the mass spectrometry investigation possible.

Conflicts of Interest: The authors declare no conflict of interest.

References

1. Marques, C.M.; Moniz, S.; de Sousa, J.P.; Barbosa-Póvoa, A.P. A simulation-optimization approach to integrate process design and planning decisions under technical and market uncertainties: A case from the chemical-pharmaceutical industry. *Comput. Chem. Eng.* **2017**, *106*, 796–813. [CrossRef]
2. Guangorena Zarzosa, G.I.; Kobayashi, T. Sustainable Polymer Used as Renewable Source for Medical Industry. In *Encyclopedia of Materials: Plastics and Polymers*; Elsevier: Amsterdam, The Netherlands, 2022; pp. 850–858. [CrossRef]
3. Santos, A.S.; Raydan, D.; Cunha, J.C.; Viduedo, N.; Silva, A.M.S.; Marques, M.M.B. Advances in green catalysis for the synthesis of medicinally relevant N-heterocycles. *Catalyst* **2021**, *11*, 1108. [CrossRef]
4. Islama, S.; Basumatary, B.; Rokhum, S.L.; Mochahari, P.; Basumatary, S. Advancement in utilization of nanomaterials as efficient and recyclable solid catalyst for biodiesel synthesis. *Chem. Eng. Technol.* **2022**, *3*, 10043. [CrossRef]
5. Bilal, M.; Ashraf, S.S.; Cui, J.; Lou, W.Y.; Franco, M.; Mulla, S.I.; Iqbal, H.M.N. Harnessing the biocatalytic attributes and applied perspectives of nanoengineered laccases—A review. *Int. J. Biol. Macromol.* **2021**, *166*, 352–373. [CrossRef]
6. Martínková, L.; Křístková, B.; Křen, V. Laccases and Tyrosinases in Organic Synthesis. *Int. J. Mol. Sci.* **2022**, *23*, 3462. [CrossRef]
7. Dăscălescu, D.; Apetrei, C. Development of a Novel Electrochemical Biosensor Based on Organized Mesoporous Carbon and Laccase for the Detection of Serotonin in Food Supplements. *Chemosensors* **2022**, *10*, 365. [CrossRef]
8. Dahiya, D.; Nigam, P.S. Sustainable Biosynthesis of Esterase Enzymes of Desired Characteristics of Catalysis for Pharmaceutical and Food Industry Employing Specific Strains of Microorganisms. *Sustainability* **2022**, *14*, 8673. [CrossRef]
9. Cardullo, N.; Muccilli, V.; Tringali, C. Laccase-mediated synthesis of bioactive natural products and their analogues. *RSC Chem. Biol.* **2022**, *3*, 614–647. [CrossRef]
10. Othman, A.M.; Sanroman, A.; Molde, D. Laccase-Oriented Immobilization Using Concanavalin A as an Approach for Efficient Glycoproteins Immobilization and Its Application to the Removal of Aqueous Phenolics. *Sustainability* **2022**, *14*, 13306. [CrossRef]
11. Osma, J.F.; Toca-Herrera, J.L.; Rodríguez-Couto, S. Cost analysis in laccase production. *J. Environ. Manag.* **2011**, *92*, 2907–2912. [CrossRef]
12. Arregui, L.; Ayala, M.; Gómez-Gil, X.; Gutiérrez-Soto, G.; Hernández-Luna, C.E.; De los Santos, M.H.; Levin, L.; Rojo-Domínguez, A.; Romero-Martínez, D.; Saparrat, M.C.N.; et al. Laccases: Structure, function, and potential application in water bioremediation. *Microb. Cell Fact.* **2019**, *18*, 200. [CrossRef]
13. Garcia-Galan, C.; Berenguer-Murcia, Á.; Fernandez-Lafuente, R.; Rodrigues, R.C. Potential of different enzyme immobilization strategies to improve enzyme performance. *Adv. Synth. Catal.* **2011**, *353*, 2885–2904. [CrossRef]
14. Petrila, L.M.; Grădinaru, V.R.; Bucatariu, F.; Mihai, M. Polymer/Enzyme Composite Materials-Versatile Catalysts with Multiple Applications. *Chemistry* **2022**, *4*, 1312–1338. [CrossRef]

15. Silva, A.R.M.; Alexandre, J.Y.N.H.; Souza, J.E.S.; Lima Neto, J.G.; de Sousa Júnior, P.G.; Rocha, M.V.P.; dos Santos, J.C.S. The Chemistry and Applications of Metal-Organic Frameworks (MOFs) as Industrial Enzyme Immobilization Systems. *Molecules* **2022**, *27*, 4529. [CrossRef]
16. Guzik, U.; Hupert-Kocurek, K.; Wojcieszynska, D. Immobilization as a strategy for improving enzyme properties- Application to oxidoreductases. *Molecules* **2014**, *19*, 8995–9018. [CrossRef]
17. Santa Cruz Matins de Queiroz, A.; Fook, B.R.P.L.; De Oliveira Lima, V.A.; De Farias Rached, R.I.; Lima, E.P.N.; Da Silva Lima, R.J.; Covas, C.A.P.; Fook, M.V.L. Preparation and characterization of chitosan obtained from shells of shrimp (Litopenaeus vannamei Boone). *Mar. Drugs* **2017**, *15*, 141. [CrossRef]
18. Mohan, K.; Ganesan, A.R.; Muralisankar, T.; Jayakumar, R.; Sathishkumar, P.; Uthayakumar, V.; Chandirasekar, R.; Revathi, N. Recent insights into the extraction, characterization, and bioactivities of chitin and chitosan from insects. *Trends Food Sci. Technol.* **2020**, *105*, 17–42. [CrossRef]
19. Mane, S.; Pathan, E.; Tupe, S.; Deshmukh, S.; Kale, D.; Ghormade, V.; Chaudhari, B.; Deshpande, M. Isolation and Characterization of Chitosans from Different Fungi with Special Emphasis on Zygomycetous Dimorphic *Fungus Benjaminiella* poitrasii: Evaluation of Its Chitosan Nanoparticles for the Inhibition of Human Pathogenic Fungi. *Biomacromolecules* **2022**, *23*, 808–815. [CrossRef]
20. Pellis, A.; Guebitz, G.M.; Nyanhongo, G.S. Chitosan: Sources, Processing and Modification Techniques. *Gels* **2022**, *8*, 393. [CrossRef]
21. Biró, E.; Németh, A.S.; Sisak, C.; Feczkó, T.; Gyenis, J. Preparation of chitosan particles suitable for enzyme immobilization. *J. Biochem. Biophys. Methods* **2008**, *70*, 1240–1246. [CrossRef]
22. Degórska, O.; Zdarta, J.; Synoradzki, K.; Zgola-Grzeskowiak, A.; Ciesielczyk, F.; Jesionowski, T. From core-shell like structured zirconia/magnetite hybrid towards novel biocatalytic systems for tetracycline removal: Synthesis, enzyme immobilization, degradation and toxicity study. *J. Environ. Chem. Eng.* **2021**, *9*, 105701. [CrossRef]
23. Wu, Y.; Guo, J.; Yang, W.; Wang, C.; Fu, S. Preparation and characterization of chitosan-poly(acrylic acid) polymer magnetic microspheres. *Polymer* **2006**, *47*, 5287–5294. [CrossRef]
24. Leonties, A.R.; Răducan, A.; Culiță, D.C.; Alexandrescu, E.; Moroșan, A.; Mihaiescu, D.E.; Aricov, L. Laccase immobilized on chitosan-polyacrylic acid microspheres as highly efficient biocatalyst for naphthol green B and indigo carmine degradation. *Chem. Eng. J.* **2022**, *439*, 135654. [CrossRef]
25. Song, X.; Chen, Y.; Zhao, G.; Sun, H.; Che, H.; Leng, X. Effect of molecular weight of chitosan and its oligosaccharides on antitumor activities of chitosan-selenium nanoparticles. *Carbohydr. Polym.* **2020**, *231*, 115689. [CrossRef] [PubMed]
26. Tai, K.; Rappolt, M.; Mao, L.; Gao, Y.; Li, X.; Yuan, F. The stabilization and release performances of curcumin-loaded liposomes coated by high and low molecular weight chitosan. *Food Hydrocoll.* **2020**, *99*, 105355. [CrossRef]
27. Ahmad, M.A.; Ahmed, N.B.; Adegoke, K.A.; Bello, O.S. Sorption studies of methyl red dye removal using lemon grass (Cymbopogon citratus). *Chem. Data Collect.* **2019**, *22*, 100249. [CrossRef]
28. Takkar, S.; Tyagi, B.; Kumar, N.; Kumari, T.; Iqbal, K.; Varma, A.; Thakur, I.S.; Mishra, A. Biodegradation of methyl red dye by a novel actinobacterium Zhihengliuella sp. ISTPL4: Kinetic studies, isotherm and biodegradation pathway. *Environ. Technol. Innov.* **2022**, *26*, 102348. [CrossRef]
29. Aricov, L.; Băran, A.; Simion, E.L.; Gîfu, I.C.; Anghel, D.F.; Jerca, V.; Vuluga, M. New insights into the self-assembling of some hydrophobically modified polyacrylates in aqueous solution. *Colloid. Polym. Sci.* **2016**, *294*, 667–679. [CrossRef]
30. Höfer, C.; Schlosser, D. Novel enzymatic oxidation of Mn^{2+} to Mn^{3+} catalyzed by a fungal laccase. *FEBS Lett.* **1999**, *451*, 186–190. [CrossRef]
31. Liu, Y.; Yan, M.; Geng, Y.; Huang, J. ABTS-modified silica nanoparticles as laccase mediators for decolorization of indigo carmine dye. *J. Chem.* **2015**, *2015*, 7. [CrossRef]
32. Aricov, L.; Leonties, A.R.; Gîfu, I.C.; Preda, D.; Raducan, A.; Anghel, D.F. Enhancement of laccase immobilization onto wet chitosan microspheres using an iterative protocol and its potential to remove micropollutants. *J. Environ. Manag.* **2020**, *276*, 111326. [CrossRef] [PubMed]
33. Solomon, E.I.; Heppner, D.E.; Johnston, E.M.; Ginsbach, J.W.; Cirera, J.; Qayyum, M.; Kieber-Emmons, M.T.; Kjaergaard, C.H.; Hadt, R.G.; Tian, L. Copper active sites in biology. *Chem. Rev.* **2014**, *114*, 3659–3853. [CrossRef]
34. Trott, O.; Olson, A.J. AutoDock Vina: Improving the speed and accuracy of docking with a new scoring function, efficient optimization, and multithreading. *J. Comput. Chem.* **2009**, *31*, 455–461. [CrossRef]
35. Piontek, K.; Antorini, M.; Choinowski, T. Crystal structure of a laccase from the fungus Trametes versicolor at 1.90-Å resolution containing a full complement of coppers. *J. Biol. Chem.* **2002**, *277*, 37663–37669. [CrossRef]
36. Frisch, M.J.; Trucks, G.W.; Schlegel, H.B.; Scuseria, G.E.; Robb, M.A.; Cheeseman, J.R.; Montgomery, J.A., Jr.; Vreven, T.; Kudin, K.N.; Burant, J.C.; et al. *Gaussian 03, Revision C.01*; Gaussian, Inc.: Wallingford, CT, USA, 2004.
37. Precupas, A.; Leonties, A.R.; Neacsu, A.; Angelescu, D.G.; Popa, V.T. Bovine hemoglobin thermal stability in the presence of naringenin: Calorimetric, spectroscopic and molecular modeling studies. *J. Mol. Liq.* **2022**, *361*, 119617. [CrossRef]
38. Varlan, A. Hillebrand, Exploring the capabilities of TDDFT calculations to explain the induced chirality upon a binding process: A simple case, 3- M. carboxycoumarin. *J. Mol. Struct.* **2013**, *1036*, 341–349. [CrossRef]
39. Morris, G.M.; Huey, R.; Lindstrom, W.; Sanner, M.F.; Belew, R.K.; Goodsell, D.S.; Olson, A.J. Software news and updates AutoDock4 and AutoDockTools4: Automated docking with selective receptor flexibility. *J. Comput. Chem.* **2009**, *30*, 2785–2791. [CrossRef]

40. Precupas, A.; Ionescu, S. Exploring the interaction of 5,6-benzocoumarin-3-carboxylic acid with bovine serum albumin at the molecular level: A biophysical investigation using molecular dynamics. *Rev. Roum. Chim.* **2021**, *66*, 49–58. [CrossRef]
41. Dassault Systèmes BIOVIA. Discovery Studio, San Diego: Dassault Systèmes. 2019. Available online: http://accelrys.com/products/discovery-studio (accessed on 3 August 2022).
42. Cerón, A.A.; Nascife, L.; Norte, S.; Costa, S.A.; do Nascimento, J.H.O.; Dal Pont Morisso, F.; Baruque-Ramos, J.; Oliveira, R.C.; Costa, S.M. Synthesis of chitosan-lysozyme microspheres, physicochemical characterization, enzymatic and antimicrobial activity. *Int. J. Biol. Macromol.* **2021**, *185*, 572–581. [CrossRef]
43. Bilal, M.; Jing, Z.; Zhao, Y.; Iqbal, H.M.N. Immobilization of fungal laccase on glutaraldehyde cross-linked chitosan beads and its bio-catalytic potential to degrade bisphenol A. *Biocatal. Agric. Biotechnol.* **2019**, *19*, 101174. [CrossRef]
44. Spinelli, D.; Fatarella, E.; di Michele, A.; Pogni, R. Immobilization of fungal (Trametes versicolor) laccase onto Amberlite IR-120 H beads: Optimization and characterization. *Process. Biochem.* **2013**, *48*, 218–223. [CrossRef]
45. Aydemir, T.; Güler, S. Characterization and immobilization of Trametes versicolor laccase on magnetic chitosan-clay composite beads for phenol removal. *Artif. Cells Nanomed. Biotechnol.* **2015**, *43*, 425–432. [CrossRef] [PubMed]
46. Christiano, C.S.; Fortes, A.L.; Daniel-da-Silva, A.M.R.B.; Xavier, A.; Tavares, P.M. Optimization of enzyme immobilization on functionalized magnetic nanoparticles for laccase biocatalytic reactions. *Chem. Eng. Process.* **2017**, *117*, 1–8. [CrossRef]
47. De Mello, M.D.; Cordeiro, D.; Costa, L.T.; Follmer, C. Catalytic properties of lipases immobilized onto ultrasound-treated chitosan supports. *Biotechnol. Bioprocess Eng.* **2013**, *18*, 1090–1100. [CrossRef]
48. Chang, M.Y.; Juang, R.S. Activities, stabilities, and reaction kinetics of three free and chitosan-clay composite immobilized enzymes. *Enzyme Microb. Technol.* **2005**, *36*, 75–82. [CrossRef]
49. Christensen, N.J.; Kepp, K.P. Setting the stage for electron transfer: Molecular basis of ABTS-binding to four laccases from Trametes versicolor at variable pH and protein oxidation state. *J. Mol. Catal. B Enzym.* **2014**, *100*, 68–77. [CrossRef]
50. Sharma, S.; Pathak, S.; Sharma, K.P. Toxicity of the azo dye methyl red to the organisms in microcosms, with special reference to the Guppy (*Poecilia reticulata* Peters). *Bull. Environ. Contam. Toxicol.* **2003**, *70*, 753–760. [CrossRef]
51. Vršanská, M.; Voběrková, S.; Jiménez, A.M.; Strmiska, V.; Adam, V. Preparation and optimisation of cross-linked enzyme aggregates using native isolate white rot fungi Trametes versicolor and Fomes fomentarius for the decolourisation of synthetic dyes. *Int. J. Environ. Res. Public Health* **2018**, *15*, 23. [CrossRef]
52. Skoronski, E.; Fernandes, M.; De Lourdes Borba Magalhães, M.; Da Silva, G.F.; João, J.J.; Soares, C.H.L.; Fúrigo Júnior, A. Substrate specificity and enzyme recycling using Chitosan immobilized laccase. *Molecules* **2014**, *19*, 16794–16809. [CrossRef]
53. Zheng, F.; Cui, B.K.; Wu, X.J.; Meng, G.; Liu, H.X.; Si, J. Immobilization of laccase onto chitosan beads to enhance its capability to degrade synthetic dyes. *Int. Biodet. Biodegrad.* **2016**, *110*, 69–78. [CrossRef]
54. Matsumoto, M.; Yamaguchi, M.; Yoshida, Y.; Senuma, M.; Takashima, H.; Kawamura, T.; Kato, H.; Takahashi, M.; Hirata-Koizumi, M.; Ono, A.; et al. An antioxidant, N,N′-diphenyl-p-phenylenediamine (DPPD), affects labor and delivery in rats: A 28-day repeated dose test and reproduction/developmental toxicity test. *Food Chem. Toxicol.* **2013**, *56*, 290–296. [CrossRef]
55. Available online: https://echa.europa.eu/documents/10162/81052d17-6bc1-972a-ebfd-7f9aa40644e7 (accessed on 3 November 2022).
56. Sari, I.P.; Simarani, K. Comparative static and shaking culture of metabolite derived from methyl red degradation by Lysinibacillus fusiformis strain W1B6. *R. Soc. Open Sci.* **2019**, *6*, 190152. [CrossRef]
57. Wong, P.K.; Yuen, P.Y. Decolourization and biodegradation of N,N′-dimethyl-p-phenylenediamine by Klebsiella pneumoniae RS-13 and Acetobacter liquefaciens S-1. *J. Appl. Microbiol.* **1998**, *85*, 79–87. [CrossRef]
58. Mittal, Y.; Dash, S.; Srivastava, P.; Mishra, P.M.; Aminabhavi, T.M.; Yadav, A.K. Azo dye containing wastewater treatment in earthen membrane based unplanted two chambered constructed wetlands-microbial fuel cells: A new design for enhanced performance. *Chem. Eng. J.* **2022**, *427*, 131856. [CrossRef]
59. Li, Z.; Lu, Y.; Wang, X.; Vekaria, A.; Jiang, M.; Zhang, H. Enhancing anthranilic acid biosynthesis using biosensor-assisted cell selection and in situ product removal. *Biochem. Eng. J.* **2020**, *62*, 107722. [CrossRef]